Classical bifurcation in a quadrupolar NMR system

A. G. Araujo-Ferreira,[1,*] R. Auccaise,[2] R. S. Sarthour,[3] I. S. Oliveira,[3] T. J. Bonagamba,[1] and I. Roditi[3]

[1]*Instituto de Física de São Carlos, Universidade de São Paulo, Caixa Postal 369, 13560-970 São Carlos, São Paulo, Brazil*

[2]*Empresa Brasileira de Pesquisa Agropecuária, Rua Jardim Botânico 1024, 22460-000 Rio de Janeiro, Rio de Janeiro, Brazil*

[3]*Centro Brasileiro de Pesquisas Físicas, Rua Dr. Xavier Sigaud 150, 22290-180 Rio de Janeiro, Rio de Janeiro, Brazil*

(Received 22 January 2013; published 8 May 2013)

The Josephson junction model is applied to the experimental implementation of classical bifurcation in a quadrupolar nuclear magnetic resonance system. There are two regimes, one linear and one nonlinear, which are implemented by the radio-frequency and the quadrupolar terms of the Hamiltonian of a spin system, respectively. These terms provide an explanation of the symmetry breaking due to bifurcation. Bifurcation depends on the coexistence of both regimes at the same time in different proportions. The experiment is performed on a lyotropic liquid crystal sample of an ordered ensemble of ^{133}Cs nuclei with spin $I = 7/2$ at room temperature. Our experimental results confirm that bifurcation happens independently of the spin value and of the physical system. With this experimental spin scenario, we confirm that a quadrupolar nuclei system could be described analogously to a symmetric two-mode Bose-Einstein condensate.

DOI: 10.1103/PhysRevA.87.053605 PACS number(s): 03.75.Mn, 05.45.Mt, 03.67.−a

The Josephson junction (JJ) model remains one of the key concepts for theoretical advances in the physics of superconductivity and superfluidity. Within the ultracold-atom scenario, the description of two-mode Bose-Einstein condensates (BEC) by means of the JJ model has afforded new insights into nonlinear tunneling [1,2], owing to nonlinearity as a source, revealing many kinds of phenomena, from entanglement to classical bifurcation [3–10]. Lately, classical bifurcation effects have attracted the attention of researchers, as they can indicate, for the associated quantum systems, a signature of quantum phase transitions [11–15] and, more recently, have been used in the study of an unstable quantum pendulum [16]. In this context and due to the huge advances in experimental control, the investigation of systems such as two BEC traps [1,5,10] or two vibrational degrees of freedom in polyatomic molecules [17–19] has become very active. The Hamiltonians modeling such systems are well described by raising and lowering operators and they may be rewritten in terms of the SU(2) operators and their commutation relations via the Schwinger pseudospin representation. In this representation, these Hamiltonians display nonlinear terms that commonly appear in the z component, as for instance in the case of a symmetric trap of a two-mode BEC. One may write the simplest Hamiltonian model as $\mathcal{H} = \chi \mathbf{J}_z^2 - \Omega \mathbf{J}_x$, where χ and Ω represent respectively the nonlinear coupling due to atom-atom interaction and the linear coupling due to an external perturbation. By this and similar models, some efforts have been made to understand the evolution of the wave function $|\Psi(t)\rangle$ in the spin-coherent representation, and to analyze entanglement [4], chaos in kicked spin systems [20], and bifurcation [21].

The Hamiltonian $\mathcal{H}$, in the nuclear magnetic resonance (NMR) scenario, has a direct physical interpretation and in the rotating frame corresponds to the Hamiltonian of a quadrupolar nuclear system acted on by a radio-frequency pulse along the negative x direction [22,23]. In this paper, we explore this equivalence of interpretation and study the feasibility of observing a signature of bifurcation in quadrupolar spin systems, while also assessing the use of the JJ model in nuclear systems.

Nuclear spin systems with $I > 1/2$ are described by the Zeeman, the quadrupolar, the radio-frequency terms, and weak interactions with, among other things, nuclei, electrons, and field fluctuations, which we refer to as an *environment term* denoted by $\mathcal{H}_{\text{env}}$ [23].

The Zeeman term is the interaction between the spin nuclear magnetic moment $-\hbar\gamma\mathbf{I} = -\hbar\gamma(\mathbf{I}_x, \mathbf{I}_y, \mathbf{I}_z)$ and a strong constant magnetic field $\mathbf{B}_0 = (0, 0, B_0)$ aligned in the z direction. The quadrupolar term is due to the interaction of the nuclear quadrupole moment (Q) with an electric field gradient (EFG) ($V_{\alpha\beta} = \partial^2 V/\partial\alpha\partial\beta$, with $\alpha, \beta = x, y, z$). This kind of interaction is a characteristic of nuclear spins with $I > 1/2$ where the EFG plays an important role. The EFG depends on the distribution of electrical charges surrounding the nucleus, which produces an electrostatic potential [$V(\mathbf{r})$]. There are two configurations of EFG, the first one a symmetric case which means that any axial orientation is equivalent ($I = 1/2$), and the other one, an asymmetric case which means that there is an axial symmetry which prevails when compared with other ones. Particularly, the present study considers an oriented system with axial symmetry; the following inequality is satisfied $|V_{zz}| \gg |V_{xx}| \approx |V_{yy}|$, which allows us to express the term as $\frac{eQV_{zz}}{4I(2I-1)}(3\mathbf{I}_z^2 - \mathbf{I}^2)$. The radio-frequency (RF) term represents the interaction between the spin nuclear magnetic moment and an external time-dependent magnetic field, which is perpendicular to the strong constant magnetic field $\mathbf{B}_0$; this term is written as $+\hbar\gamma B_1[\mathbf{I}_x \cos(\omega_{RF} t + \phi) + \mathbf{I}_y \sin(\omega_{RF} t + \phi)]$, where the phase ϕ defines its direction on the xy plane. In a rotating frame, the NMR Hamiltonian is given by

$$\mathcal{H}_{\text{NMR}} = -\hbar(\omega_L - \omega_{RF})\mathbf{I}_z + \hbar\frac{\omega_Q}{6}\left(3\mathbf{I}_z^2 - \mathbf{I}^2\right) + \hbar\omega_1(\mathbf{I}_x \cos\phi + \mathbf{I}_y \sin\phi) + \mathcal{H}'_{\text{env}}, \quad (1)$$

where $\omega_Q = \frac{3eQV_{zz}}{2I(2I-1)\hbar}$ represents the quadrupolar coupling, $\omega_1 = \gamma B_1$ is the RF strength, and $\omega_L = \gamma B_0$ the Larmor

*avatar@ifsc.usp.br

frequency of a nuclear species. The Larmor frequency and quadrupolar coupling satisfy the inequality $|\omega_L| \gg |\omega_Q|$.

To match the Hamiltonian $\mathcal{H}$ and the NMR Hamiltonian $\mathcal{H}_{\rm NMR}$, let us choose $\omega_{RF} = \omega_L$ and $\phi = \pi$, such that, without loss of generality, we may drop the constant term $-\frac{\hbar\omega_Q}{6}\mathbf{I}^2$ and the environment term $\mathcal{H}'_{\rm env}$. Now the NMR Hamiltonian takes the form $\mathcal{H}_{\rm NMR} = \frac{\hbar\omega_Q}{2}\mathbf{I}_z^2 - \hbar\omega_1\mathbf{I}_x$. Next, by substituting the dimensionless parameter $\Lambda = \frac{I\omega_Q}{\omega_1}$ the NMR Hamiltonian can be rewritten:

$$\mathcal{H}'_{\rm NMR} = \frac{\mathcal{H}_{\rm NMR}}{\hbar\omega_1} = \frac{\Lambda}{2I}\mathbf{I}_z^2 - \mathbf{I}_x. \tag{2}$$

We then use this Hamiltonian to look into the classical bifurcation mechanism in nuclear spin systems. The corresponding semiclassical Hamiltonian is generated by mapping the quantum mechanical operators onto the complex numbers, following the usual procedure reported in [3,21]. This amounts to letting $\mathbf{I}_z \to z$ and $\mathbf{I}_x \to \sqrt{1-z^2}\cos\zeta$, giving

$$\mathcal{H}' = \frac{\Lambda}{2}z^2 - \sqrt{1-z^2}\cos\zeta, \tag{3}$$

where, for our purposes, z represents the temporal mean z magnetization and ζ a relative phase. In classical mechanics, Eq. (3) describes the motion of a particle in a phase potential defined by $V(\zeta) = -\sqrt{1-z^2}\cos\zeta$, where V is shaped by $\cos\zeta$ and weighted by $\sqrt{1-z^2}$ as sketched in Fig. 1(a). Λ is a tunable parameter that determines the dynamics of a particle in a conserved energy configuration. From Hamilton's equations of motion $\dot{z} = -\partial\mathcal{H}'/\partial\zeta$ and $\dot{\zeta} = \partial\mathcal{H}'/\partial z$ we have

$$\dot{z} = -\sqrt{1-z^2}\sin\zeta, \tag{4}$$

$$\dot{\zeta} = \Lambda z + \frac{z}{\sqrt{1-z^2}}\cos\zeta, \tag{5}$$

such that z and ζ are canonically conjugate variables. The fixed points of the Hamiltonian $\mathcal{H}'$, denoted by $P = (z_0,\zeta_0)$, are determined by the condition $\dot{z} = \dot{\zeta} = 0$. These are $\zeta_0 = \pm n\pi$ with $n = 0,1,2,\ldots$ and $z_0 = \{0, \pm\sqrt{1-1/\Lambda^2}\}$. Note that there are many interesting sets of fixed points to analyze. The trivial one, $P_0 = (0,0)$, which corresponds to a stable fixed point, is located on the positive X axis of the coordinate frame [see Fig. 1(b)]. Physically, in the NMR scenario, it corresponds to an extreme situation of null quadrupolar coupling, or to a linear regime ($\Lambda < 1$). Still in the linear regime, $P_\pi = (0,\pi)$ matches another stable fixed point, located on the negative X axis of the coordinate frame [see Fig. 1(b)]. The nontrivial fixed points are $P_\pm = (\pm\sqrt{1-1/\Lambda^2},\pi)$; here, for $\Lambda > 1$, it can be seen that the stable fixed point P_π undergoes a supercritical Pitchfork bifurcation, becoming unstable, and it splits up into two others, the $P_\pm$ stable fixed points. These are divided by a separatrix in Fig. 1(b). In the NMR interpretation, this picture corresponds to the situation of a quadrupolar coupling stronger than the RF pulse intensity, or to a nonlinear regime. Our efforts were focused on finding out how this theoretical analysis could be reached by using nuclear spin systems.

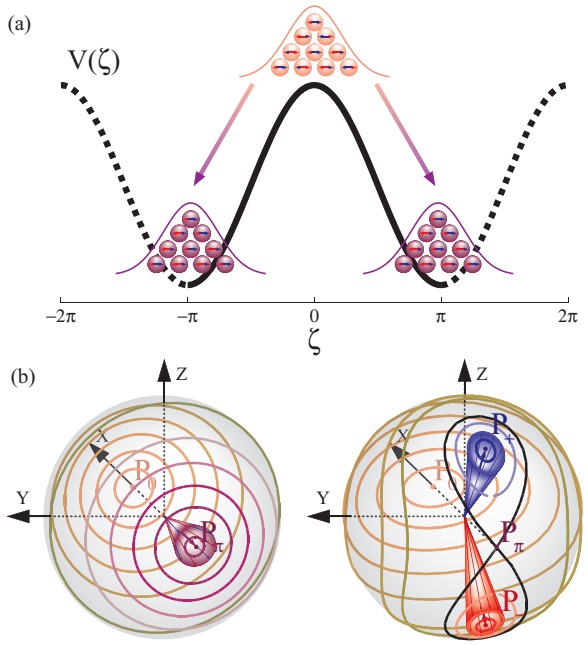

FIG. 1. (Color online) Sketch of the spin scenario of the bifurcation process discussed in this paper. (a) Initially the spin state precesses around fixed point P_0, such that after the dynamics the spin system goes to one of the points $P_\pm$ depending on the value of Λ. (b) Trajectories drawn on the spherical phase space before and after the bifurcation process that depends on the value of Λ. Left frame represents trajectories at a linear regime which happens at $0 \leqslant \Lambda \leqslant 1$ and right frame represents trajectories at nonlinear regime corresponding to $1 \leqslant \Lambda$. The typical supercritical pitchfork bifurcation scenario occurs; i.e., a stable fixed point bifurcates into two new stable fixed points while the original becomes unstable.

The spin scenario and the experimental implementations were performed in a lyotropic liquid crystal sample prepared with 42.5 wt % cesium–pentadecafluoroctanoate (Cs-PFO) and 57.5 wt % deuterated water (D_2O) [24]. Cesium nuclei (^{133}Cs) are quadrupolar spin systems with $I = 7/2$ such that the dimension of the Hilbert space is $d = 2I + 1 = 8$. The experiment was carried out in a Varian 500 MHz premium shielded (11.7 T) spectrometer at room temperature (25 °C). A liquid NMR 5 mm probe was used in this experiment. The Larmor frequency and quadrupolar coupling are 65.598 MHz and 7.7 kHz, respectively. The π-pulse time was calibrated as 25 μs. The spin-lattice and spin-spin relaxation time, for cesium nuclei, is $T_1 \approx$ 320 ms and $T_2 \approx$ 4 ms, respectively. The recycle delay time is d_1 = 1.8 s.

To describe a quantum state in NMR implementations, we use the density operator formalism representing the thermal equilibrium state, whose populations satisfy the Boltzman-Gibbs distribution. Theoretically, the density operator is represented by $\rho = \frac{1}{\mathcal{Z}}\exp[-\beta\mathcal{H}_0]$, where $\mathcal{H}_0 = -\hbar\omega_L\mathbf{I}_z$ is the secular contribution of the NMR Hamiltonian and $\beta = (k_BT)^{-1}$, k_B being the Boltzmann constant and T the room temperature. If the polarization strength is $\epsilon = \beta\omega_L\hbar/\mathcal{Z}$, where $\mathcal{Z}$ is the partition function, and this factor has a value $\sim 10^{-5}$ then the density operator could be expanded to a first-order approximation as $\rho = \frac{1}{\mathcal{Z}}\mathbf{1} + \epsilon\rho_0$, in which $\rho_0 = \mathbf{I}_z$ is called the deviation density matrix.

To initialize the quantum state, we transform ρ_0 to prepare a pseudo–nuclear spin coherent state (pseudo–NSCS) using the protocol of Refs. [25,26]. This is a coherent state implemented experimentally in a nuclear spin system. The pseudo-NSCS is

denoted as $|\zeta(\theta,\varphi)\rangle$, so the density operator is $\rho = (\frac{1}{8} - \epsilon)\mathbf{1} + \epsilon\Delta\rho$, such that $\Delta\rho \equiv |\zeta(\theta,\varphi)\rangle\langle\zeta(\theta,\varphi)|$, for any $0 \leqslant \theta \leqslant \pi$ and $0 \leqslant \varphi \leqslant 2\pi$.

For our purpose, the angular parameters (polar θ and azimuthal φ) of a pseudo-NSCS were chosen in such a way that the phenomenon of bifurcation appeared as sharply as possible and therefore these parameters were fixed at a pair of initial conditions $|\zeta_+(\pi/4,\pi)\rangle$ and $|\zeta_-(3\pi/4,\pi)\rangle$, where the ζ positive (ζ negative) represents an initial condition at the north (south) hemisphere of a spherical phase space.

To sketch the classical bifurcation, we must monitor the quantum dynamics of an initial quantum state of the spin system under the effect of the Hamiltonian (2) at different τ values and Λ values to establish a temporal mean value of an observable of the spin system. In the NMR scenario, the observable of interest is the quantum dynamics of $\mathbf{I}_z$ under different (Λ,τ) values and the temporal mean z magnetization is the main physical quantity to observe, denoted by $z(\Lambda) = \sum_\tau \langle \mathbf{I}_z(\Lambda,\tau)\rangle$. So, we use a control parameter Λ, such that ω_Q is maintained at a constant strength and ω_1 is varied from highest to lowest values. The different strengths of ω_1 are quantified by the calibration of π pulses at various elapsed times $t_\pi = 25, 30, 40, 50, 60, 100\ \mu$s or for the parameter $\Lambda = 0.67, 0.81, 1.08, 1.35, 1.62, 2.70$. Once we have chosen the strength of ω_1, the implemented pseudo-NSCS $|\zeta_\pm(\theta,\varphi)\rangle$ is transformed by a RF pulse that depends on the Hamiltonian in Eq. (2) at various times $\tau = k\Delta\tau$ and $k = 0,\ldots,44$ with $\Delta\tau = 5\ \mu$s. At each step, the pseudo-NSCS is tomographed by the quantum state tomography (QST) procedure [26,27]. QST enables us to reconstruct the deviation density matrix $(\Delta\rho)$ corresponding to the last stage of the system evolution. It comprises essentially the application of a set of rotations on the different spins that allows us to reconstruct the density matrix from the measured NMR spectra. Using this experimental tool, it is possible to obtain information about any desired observable of the spin system at different τ values. Next, the average value of the z component of the spin angular momentum, $\langle \mathbf{I}_z(\Lambda,\tau)\rangle = \mathrm{Tr}\{\Delta\rho(\Lambda,\tau)\ \mathbf{I}_z\}$, is computed.

In the top (bottom) of Fig. 2 we show the experimental results for z magnetization and its distribution for initial conditions on the north (south) hemisphere of the spherical phase space under the linear (nonlinear) regime. On the left of Fig. 2(a) are shown experimental (dots) and numerical (solid line) results for $\langle \mathbf{I}_z(\Lambda,\tau)\rangle$, for the initial condition on the north hemisphere under the linear regime, but not too far from the nonlinear regime, such that $\Lambda \approx 0.67$. The beats and fast decay are a typical signature of an intermediate regime. Notice that we are using a numerical procedure to verify the fidelity of our experimental results. To explain this procedure, let us consider the first experimental quantum state $\Delta\rho = |\zeta_+\rangle\langle\zeta_+|$ at $\tau = 0$ gotten by the QST which corresponds at north hemisphere under the spherical phase space. Next, we transform it by an operator that depends on $\mathcal{H}'_{\mathrm{NMR}}$ [see Eq. (2)] at different τ values, such as it happens at quasi-continuous τ values. The first magnetization value $\langle \mathbf{I}_z(0)\rangle$ is denoted by a blue circle in Fig. 2(a) and the continuous line represent z magnetization computed from the evolution of $\Delta\rho(\Lambda,\tau) = \exp[-i\hbar\omega_1\mathcal{H}'_{\mathrm{NMR}}\tau]\,\Delta\rho\,\exp[i\hbar\omega_1\mathcal{H}'_{\mathrm{NMR}}\tau]$. We stress the fact that we are not using any method of fitting and/or interpolation to predict the experimental data; we

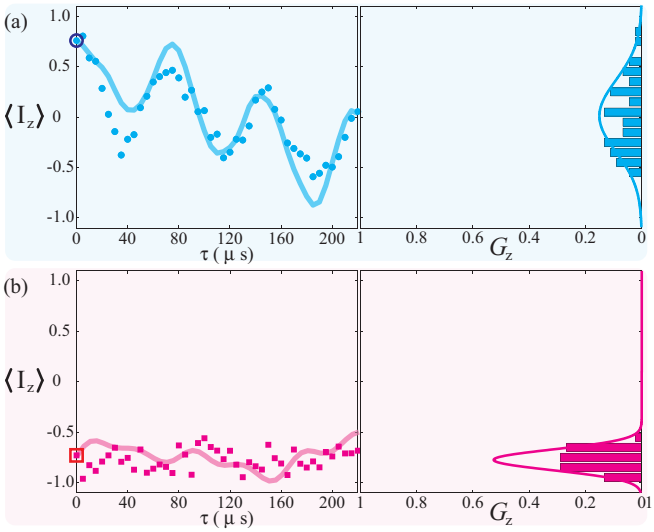

FIG. 2. (Color online) Experimental results (symbols) and numerical results (continuous lines) for the dynamics of mean average values of $\langle \mathbf{I}_z(\Lambda,\tau)\rangle$-magnetization (left) and its $\langle \mathbf{I}_z(\Lambda,\tau)\rangle$-magnetization distribution (right). Each value was calculated from the tomographed deviation density matrix at 45 different values of τ. Results for (a) initial condition on north hemisphere and a linear regime, (b) initial condition on south hemisphere and a nonlinear regime.

only are predicting the behavior of magnetization through the natural quantum evolution of the spin system. On the right of Fig. 2(a) we display a histogram of the experimental values of $\langle \mathbf{I}_z(\tau)\rangle$ and the Gaussian distribution $G_z(\langle \mathbf{I}_z\rangle) = G_0 \exp[-(\langle \mathbf{I}_z\rangle - z)^2/\sigma_z^2]$ has been calculated and drawn. The parameter $z(0.67)$, referred to as the temporal mean z magnetization, corresponds to the mean value of $\langle \mathbf{I}_z(\Lambda,\tau)\rangle$ over 45 different elapsed time points. Similarly, the parameter σ_z is the well-known standard deviation. The main information extracted from G_z is the z value, which depends on Λ, and this parameter indicates the stage of bifurcation.

On the left of Fig. 2(b) we show experimental (squares) and numerical (solid line) results for $\langle \mathbf{I}_z(\Lambda,\tau)\rangle$ in the nonlinear regime, satisfying $\Lambda = 2.7 > 1$. The red square represents the initial z magnetization computed from the initial quantum state $\Delta\rho = |\zeta_-\rangle\langle\zeta_-|$ at $\tau = 0$ read out by the QST which corresponds at south hemisphere under the spherical phase space, and the continuous line represent prediction using numerical procedures, as explained above. The smooth beats are almost completely attenuated and the decay is slower than in the linear regime. This happens because ω_1 is weaker than ω_Q. On the right of Fig. 2(b), there is a histogram for experimental values of $\langle \mathbf{I}_z(\tau)\rangle$ and a Gaussian distribution $G_z(\langle \mathbf{I}_z\rangle)$.

In Fig. 3 we present the experimental results (symbols) and theoretical prediction (solid lines) of the temporal mean z magnetization for initial conditions on the north hemisphere (dots) and south hemisphere (squares). The cyan circle (magenta square) indicates that the data were calculated from experimental results explained in Fig. 2(a) [Fig. 2(b)]. We observe that the experimental results match the theoretical prediction of bifurcation. To explain this phenomenon in a nuclear spin system, we need to remember that the eigenstates of the secular

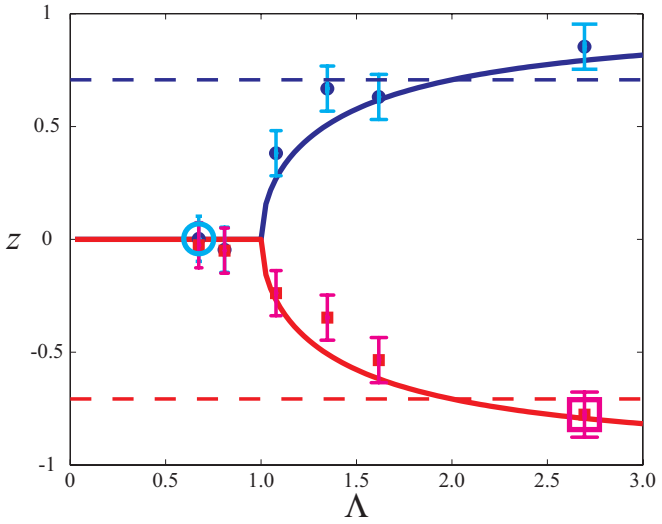

FIG. 3. (Color online) Experimental results (symbols) of bifurcation phenomena in spin systems which are described by the JJ model. Two initial conditions are denoted by dashed lines, which correspond to $|\zeta_+\rangle$ and $|\zeta_-\rangle$ pseudo-NSCS. The spin system can be driven under different regimes: a linear ($0 < \Lambda < 1$) and a nonlinear ($1 < \Lambda$). Theoretical predictions (solid lines) are sketched by using $\pm\sqrt{1 - 1/\Lambda}$, whose positive (negative) sign corresponds to the north (south) hemisphere of a spherical phase space. The cyan circle (magenta square) indicates that the data were calculated from experimental results explained in Fig. 2(a) [Fig. 2(b)]. The error bars are bounded at 10% of the maximum value of the time-averaged z magnetization, which is $|\pm 1|$.

Hamiltonian are $|m\rangle$, with $m = -I, -I+1, \ldots, I-1, I$, and the operator that depends on Hamiltonian (2) transforms each eigenstate. In the linear regime, the RF term imposes the dynamics of spins, maintaining the spin system under a superposition of the $|m\rangle$ eigenstates, leading the quantum state from $|\zeta_+\rangle$ to $|\zeta_-\rangle$ and vice versa. This is analogous to what happens in the tunneling phenomenon of a symmetrical trap of a two-mode BEC [1–5,9,10,12–15] or what happens in the description of the JJ model in superconductivity, called the plasma oscillation regime [2]. On the other hand, in the nonlinear regime, the nonlinear term decides the behavior of the system. In this case, from the basic principles of quantum mechanics, we know that $\mathbf{I}_z^2 |\pm m\rangle = \hbar m^2 |\pm m\rangle$; for $|+m\rangle$ and $|-m\rangle$ there is a degeneracy which drives the spin system to the bifurcation phenomenon, because the initial condition for the north (south) hemisphere is retained by the operator that depends on Hamiltonian (2) and the spin system is induced to precess aligned parallel (antiparallel) to an effective magnetic field which is aligned along the z axis of a reference frame. Similarly, in a two-mode BEC, this regime corresponds to the self-trapping regime [2].

On the other hand, the analogous small number of particles on a quadrupolar NMR system satisfies limits established by studies on two mode BEC systems. In fact, the inequality established by Eq. (13) of Ref. [28] provides us an insight, upon typical values for ultracold Bose systems, such that $N \ll 200$, where N is the number of particles. In the case of $N = 2I$ for any quadrupolar nuclei system, this inequality is satisfied.

Our data show that even for $I = 7/2$, which does not correspond to a very large N, the quadrupolar system provides a good picture of the behavior of the two-mode Hamiltonian in the classical regime described by Eq. (3). Here, we stress again that these data are obtained by applying the evolution operator based on the full quantum Hamiltonian given by Eq. (2). What happens is that in our case, the semiclassical approximation is guaranteed by the depletion condition of the Bogoliubov formalism [30] which means that for the total number of particles of the system (N), the ground state is occupied by N_0 particles such that $N_0 \sim N$. In other words, if it is possible to leave the quantum state of the particles system onto a coherent state [28] or to establish an order parameter [11] then the semiclassical approximation will be satisfied. This condition is achieved in a quadrupolar system when the pseudo-NSCS [25] is implemented; in that case the collective behavior of the analogous $2I$ particles is attached to the ground state.

It is worthy of notice here that in a quantum simulation scenario, in the case of quantum information processing, an invertible map is needed to transform from the Hamiltonian of the quantum simulator onto the Hamiltonian of the physical system and vice versa [29]. In the present study we are not using that kind of mapping; hence we are not dealing with that simulation scenario. Our results express essentially the analogy between orbital angular momentum operators (**J**'s) and nuclear spin angular momentum operators (**I**'s) at the level of their Lie algebra properties.

Finally, we draw our conclusions: We performed a classical bifurcation in a nuclear spin system that is described and interpreted by the JJ model. The spin scenario coincides with other experimental schemes commonly named as the symmetric double-well trap of the two-mode BEC, with the possibility of extending to the asymmetric case. We take advantage of the main physical property of a lyotropic liquid crystal sample, which is the collective order in the presence of a magnetic field. This inspired us to explore the nonlinear regime to study squeezing processes, which are currently being developed in our laboratory.

The authors acknowledge financial support from CNPq, CAPES, FAPESP, and FAPERJ. This work was performed as part of the Brazilian National Institute of Science and Technology for Quantum Information (INCT-IQ). We also acknowledge P. Judeinstein for Cs-PFO samples and thank Angela Foerster for meaningful discussions and suggestions.

[1] M. Albiez, R. Gati, J. Folling, S. Hunsmann, M. Cristiani, and M. K. Oberthaler, Phys. Rev. Lett. **95**, 010402 (2005).

[2] R. Gati and M. K. Oberthaler, J. Phys. B: At. Mol. Opt. Phys. **40**, R61 (2007).

[3] S. Raghavan, A. Smerzi, S. S. Fantoni, and S. R. Shenoy, Phys. Rev. A **59**, 620 (1999).

[4] A. S. Sorensen and K. Molmer, Phys. Rev. Lett. **86**, 4431 (2001).

[5] Michael E. Kellman and Vivian Tyng, Phys. Rev. A **66**, 013602 (2002).
[6] G. Santos, A. Tonel, A. Foerster, and J. Links, Phys. Rev. A **73**, 023609 (2006).
[7] A. Tonel, J. Links, and A. Foerster, J. Phys. A **38**, 1235 (2005).
[8] J. Links, A. Foerster, A. Tonel, and G. Santos, Annales Henri Poincaré **7**, 1591 (2006).
[9] Andrew P. Hines, Ross H. McKenzie, and G. J. Milburn, Phys. Rev. A **71**, 042303 (2005).
[10] T. Zibold, E. Nicklas, C. Gross, and M. K. Oberthaler, Phys. Rev. Lett. **105**, 204101 (2010).
[11] E. R. F. Ramos, L. Sanz, V. I. Yukalov, and V. S. Bagnato, Phys. Rev. A **76**, 033608 (2007).
[12] V. S. Shchesnovich and V. V. Konotop, Phys. Rev. Lett. **102**, 055702 (2009).
[13] B. Julia-Diaz, D. Dagnino, M. Lewenstein, J. Martorell, and A. Polls, Phys. Rev. A **81**, 023615 (2010).
[14] B. Julia-Diaz, J. J. Martorell, and A. Polls, Phys. Rev. A **81**, 063625 (2010).
[15] D. Rubeni, A. Foerster, E. Mattei, and I. Roditi, Nucl. Phys. B **856**, 698 (2012).
[16] C. S. Gerving, T. M. Hoang, B. J. Land, M. Anquez, C. D. Hamley, and M. S. Chapman, Nat. Commun. **3**, 1169 (2012).
[17] Kevin K. Lehmann, J. Chem. Phys. **79**, 1098 (1983).
[18] Michael E. Kellman, Chem. Phys. Lett. **113**, 489 (1985).
[19] Zhiming Li, Lin Xiao, and Michael E. Kellman, J. Chem. Phys. **92**, 2251 (1990).
[20] K. Nakamura, Y. Okazaki, and A. R. Bishop, Phys. Rev. Lett. **57**, 5 (1986).
[21] A. Smerzi, S. Fantoni, S. Giovanazzi, and S. R. Shenoy, Phys. Rev. Lett. **79**, 4950 (1997).
[22] I. S. Oliveira *et al.*, *NMR Quantum Information Processing* (Elsevier, Amsterdam, 2007).
[23] Charles P. Slichter, *Principles of Magnetic Resonance*, 3rd enlarged ed. (Springer, Berlin, Heidelberg, New York, 1992).
[24] N. Boden, K. W. Jolley, and M. H. Smith, J. Phys. Chem. **97**, 7678 (1993).
[25] R. Auccaise, E. R. de Azevedo, E. I. Duzzioni, T. J. Bonagamba, and M. H. Y. Moussa, arXiv:1301.2862.
[26] A. G. Araujo-Ferreira *et al.*, Int. J. Quantum. Inform. **10**, 1250016 (2012).
[27] J. Teles *et al.*, J. Chem. Phys. **126**, 154506 (2007).
[28] G. J. Milburn, J. Corney, E. M. Wright, and D. F. Walls, Phys. Rev. A **55**, 4318 (1997).
[29] S. Somaroo, C. H. Tseng, T. F. Havel, R. Laflamme, and D. G. Cory, Phys. Rev. Lett. **82**, 5381 (1999).
[30] Alexander L. Fetter and John Dirk Walecka, *Quantum Theory of Many-Particle Systems*, 1st ed. (McGraw-Hill, San Francisco, 1971).